Structural parameters of twist-bend nematics and splay-bend nematics in Dozov's theory

Michał Szmigielski[*] and Mariola Buczkowska

Institute of Physics, Lodz University of Technology, ulica Wólczańska 217/221, 93-005 Łódź, Poland

This paper presents the results of numerical calculations revealing how the structural parameters (i.e., the pitch p_{TB}, the spatial period p_{SB}, and the tilt angle θ_{TB} or θ_{SB}) of twist-bend nematics (N_{TB}) and splay-bend nematics (N_{SB}) depend on the values of elastic constants in Dozov's theory [I. Dozov, Europhys. Lett. **56**, 247 (2001)]. Alternative formulas for p_{TB}, θ_{TB}, p_{SB}, and θ_{SB} have been derived and it has been proved that they give more accurate results than the expressions proposed by Dozov. Although the determination of the fourth-order elastic constants C_1, C_2, and C_3 is not feasible in a simple way, the order of magnitude of the sum $C_1 + C_2$ has been easily estimated and is equal to 10^{-31} J m. Moreover, the numerical calculations have shown that twist-bend nematics can exist even when K_{11} is smaller than $2K_{22}$ and thus Dozov's criterion $K_{11} > 2K_{22}$ for the stability of the N_{TB} phase is not strictly satisfied.

I. INTRODUCTION

According to numerous studies, banana-shaped molecules can form nematic liquid-crystalline phases with periodically modulated structure [1–3]. One of them is a twist-bend nematic phase (N_{TB}), in which twist and bend deformations coexist spontaneously. The director field $\mathbf{n_{TB}}$ characterizing the N_{TB} structure is given in the Cartesian coordinate system xyz by the following formula:

$$\mathbf{n_{TB}} = \sin\theta_{TB}\cos q_{TB}z\hat{\mathbf{x}} + \sin\theta_{TB}\sin q_{TB}z\hat{\mathbf{y}} + \cos\theta_{TB}\hat{\mathbf{z}}. \quad (1)$$

Equation (1) describes the heliconical modulation of the director distribution in twist-bend nematics. This means that the director $\mathbf{n_{TB}}$ is twisted around a certain direction in the space (in this case the z axis of the coordinate system). The angle θ_{TB} between $\mathbf{n_{TB}}$ and $\hat{\mathbf{z}}$ is smaller than 90° and is called the tilt angle or the heliconical angle. The spatial period p_{TB} of the N_{TB} phase (commonly termed the pitch) does not usually exceed several nanometers which is the length of a few molecules [4,5]. The quantity $q_{TB} = 2\pi/p_{TB}$ is the wave number of the N_{TB} structure.

The other liquid-crystalline phase which has been theoretically predicted for highly curved molecules is splay-bend nematic (N_{SB}). In this structure periodic splay and bend distortions take place and the director field $\mathbf{n_{SB}}$ can be expressed as follows:

$$\mathbf{n_{SB}} = \sin(\theta_{SB}\sin q_{SB}z)\hat{\mathbf{y}} + \cos(\theta_{SB}\sin q_{SB}z)\hat{\mathbf{z}}, \quad (2)$$

where θ_{SB} is the maximum tilt angle of the director and q_{SB} is the wave number of the N_{SB} phase.

Experiments confirm that the N_{TB} phase is exhibited in the bounded temperature range by many liquid-crystalline compounds (for example, CB7CB [6], CB9CB [7], CB6OCB [8], and DTC5C7, DTC5C9, and DTC5C11 [9]). It should

be noted that this fact is questioned by Samulski and his co-workers [10,11]. These researchers believe that the experimental results are misinterpreted and twist-bend nematics have not been discovered yet. However, the argumentation presented in [10,11] has not found acceptance in the scientific community [12]. For this reason we treat the experimental results as convincing evidence of the existence of the N_{TB} phase.

Compared to twist-bend nematics, the splay-bend nematic phase is more elusive and exists only under specific conditions. It has been shown that the director distribution characteristic of splay-bend nematics can be induced in the N_{TB} phase by a strong electric field [13–15]. Moreover, the N_{SB} structure has been identified in colloidal systems [16] as well as in defect walls separating domains of opposite handedness in twist-bend nematics [17]. Until now, the observations have not revealed the transition to the splay-bend nematic phase occurring in thermotropic liquid crystals as a result of the temperature change [15,18].

The elastic properties of twist-bend nematics and splay-bend nematics can be described within the frame of numerous theories [2,13,18–26]. One of the first elasticity models was proposed by Dozov in 2001 [2]. In his theory the free energy density of a liquid crystal is given by the following formula,

$$\begin{aligned}
f = \frac{1}{2}\{&K_{11}[\mathbf{n}(\nabla\cdot\mathbf{n})]^2 + K_{22}[\mathbf{n}\cdot(\nabla\times\mathbf{n})]^2 \\
&+ K_{33}[\mathbf{n}\times(\nabla\times\mathbf{n})]^2\} + \frac{1}{4}\left\{C_1\sum_{l=1}^{3}\sum_{k=1}^{3}\left[\frac{d^2}{dz^2}(n_l n_k)\right]^2\right. \\
&\left.+ 2C_2\sum_{k=1}^{3}\left[\frac{d^2}{dz^2}(n_3 n_k)\right]^2 + C_3\left[\frac{d^2}{dz^2}(n_3^2)\right]^2\right\}, \quad (3)
\end{aligned}$$

where K_{11} is the splay elastic constant; K_{22} is the twist elastic constant; K_{33} is the bend elastic constant; and C_1, C_2, and

———————
[*]michal.szmigielski@dokt.p.lodz.pl

C_3 are fourth-order elastic constants. In order to decrease the number of unknown coefficients, it has been assumed that the director distribution depends only on one coordinate.

Based on his theory, Dozov derives the formulas for the characteristic parameters (i.e., the tilt angle and the wave number) of both phases—twist-bend nematics and splay-bend nematics [2]. For the N_{TB} structure he obtains

$$\theta_{TB}^2 = -\frac{K_{33}}{3K_{22}}, \tag{4}$$

$$q_{TB}^2 = -\frac{K_{33}}{3(C_1 + C_2)}. \tag{5}$$

In the case of the N_{SB} phase, his calculations yield

$$\theta_{SB}^2 = -\frac{4K_{33}}{3K_{11}}, \tag{6}$$

$$q_{SB}^2 = -\frac{K_{33}}{3(C_1 + C_2)}. \tag{7}$$

According to Dozov's theory, the twist-bend nematic and splay-bend nematic phases can be formed only if $K_{33} < 0$. The type of appearing structure depends on the values of K_{11} and K_{22}. When the condition

$$K_{11} > 2K_{22} \tag{8}$$

is satisfied, the N_{TB} phase is energetically favorable; otherwise the N_{SB} phase should be stable [2].

It must be mentioned that Eqs. (4)–(8) have been derived after introducing some simplifications. For instance, small values of the tilt angle have been assumed. The aim of this paper is to verify the formulas (4)–(7) and the criterion (8) by means of numerical calculations. It will be established how the tilt angle and the wave number depend on the material parameters used in Dozov's model for twist-bend nematics and splay-bend nematics. The additional purpose of the research is to estimate the order of magnitude of C_1, C_2, and C_3 on the basis of computations.

II. METHODS

The equilibrium values of the tilt angle and the wave number of twist-bend nematics or splay-bend nematics correspond to the minimum of the free energy density. In Dozov's theory the formula for the free energy density of the N_{TB} phase can be obtained by the substitution of (1) into (3):

$$f_{TB} = \tfrac{1}{2}K_{22}q_{TB}^2\sin^4\theta_{TB} + \tfrac{1}{2}K_{33}q_{TB}^2\cos^2\theta_{TB}\sin^2\theta_{TB}$$
$$+ \tfrac{1}{2}(C_1 + C_2)q_{TB}^4\cos^2\theta_{TB}\sin^2\theta_{TB} + 2C_1q_{TB}^4\sin^4\theta_{TB}. \tag{9}$$

Using Eqs. (2) and (3), one can write the analogous expression for the N_{SB} structure:

$$f_{SB} = \tfrac{1}{2}q_{SB}^2\theta_{SB}^2\cos^2 q_{SB}z[K_{11}\sin^2(\theta_{SB}\sin q_{SB}z) + K_{33}\cos^2(\theta_{SB}\sin q_{SB}z)] + \tfrac{1}{2}(C_1 + C_2)\left(q_{SB}^4\theta_{SB}^2\sin^2 q_{SB}z + 4q_{SB}^4\theta_{SB}^4\cos^4 q_{SB}z\right)$$

$$+ C_3q_{SB}^4\theta_{SB}^4\cos^4 q_{SB}z\cos^2(2\theta_{SB}\sin q_{SB}z) + \tfrac{1}{4}C_3q_{SB}^4\theta_{SB}^2\sin^2 q_{SB}z\sin^2(2\theta_{SB}\sin q_{SB}z)$$

$$- C_3q_{SB}^4\theta_{SB}^3\cos^2 q_{SB}z \sin q_{SB}z \cos(2\theta_{SB}\sin q_{SB}z)\sin(2\theta_{SB}\sin q_{SB}z). \tag{10}$$

For twist-bend nematics, the parameters θ_{TB} and q_{TB} are found by the numerical minimization of formula (9). The procedure is based on the method of steepest descent [27]. It is one of the simplest gradient-based optimization algorithms. In every iteration the starting point is the current approximation of the minimum $\mathbf{x}^{[k]} = [\theta_{TB}^{[k]}, q_{TB}^{[k]}]$, where k is the step number. On this basis the antigradient $\mathbf{d}^{[k]} = -\nabla f_{TB}(\mathbf{x}^{[k]}) = [-\frac{\partial f_{TB}}{\partial \theta_{TB}}|_{\theta_{TB}^{[k]}, q_{TB}^{[k]}}, -\frac{\partial f_{TB}}{\partial q_{TB}}|_{\theta_{TB}^{[k]}, q_{TB}^{[k]}}]$ is calculated because in this direction f_{TB} decreases fastest. The new approximation of the minimum is equal to $\mathbf{x}^{[k+1]} = \mathbf{x}^{[k]} + \alpha^{[k]}\mathbf{d}^{[k]}$. The parameter $\alpha^{[k]} > 0$ is found by the minimization of $f_{TB}(\mathbf{x}^{[k]} + \alpha^{[k]}\mathbf{d}^{[k]})$. For this purpose the technique of the golden-section search is applied. The iterations are interrupted when the norm of the difference $\mathbf{x}^{[k+1]} - \mathbf{x}^{[k]}$ is sufficiently small. The initial approximation $\mathbf{x}^{[0]} = [\theta_{TB}^{[0]}, q_{TB}^{[0]}]$, which is necessary for starting the computations, is chosen by trial and error since not every choice ensures the good convergence of the algorithm.

In the case of splay-bend nematics, the numerical problem is more complicated because the free energy density given by Eq. (10) depends on the spatial coordinate z. This creates the necessity of considering one period ($p_{SB} = 2\pi/q_{SB}$) of the N_{SB} structure, over which the free energy density needs to be

integrated and then averaged. As a result of these operations, the following quantity is calculated:

$$\langle F_{SB} \rangle = \frac{1}{p_{SB}}\int_0^{p_{SB}} f_{SB}dz = \frac{q_{SB}}{2\pi}\int_0^{p_{SB}} f_{SB}dz. \tag{11}$$

Because the formula for f_{SB} is complex, the computation of $\langle F_{SB} \rangle$ is performed numerically in the way described below. Firstly, the area of integration must be discretized and therefore the set of evenly spaced and numbered nodes is generated. The distance Δz between two adjacent nodes is equal to

$$\Delta z = \frac{p_{SB}}{N - 1} = \frac{2\pi}{q_{SB}(N - 1)}, \tag{12}$$

where N is the total number of nodes. The spatial coordinate z_i of the node with number i is given by

$$z_i = \frac{2\pi i}{q_{SB}(N - 1)}. \tag{13}$$

It has been assumed that the zeroth node ($i = 0$) is situated in the origin of the coordinate system ($z = 0$). The next step is to transform the integral in Eq. (11) into the sum over discrete elements. For this purpose the continuous spatial coordinate

z is replaced with z_i and Δz is introduced instead of the differential dz. Moreover, it must be taken into account that the elements connected with the boundary nodes ($i = 0$ and $i = N-1$) have the length of $\Delta z/2$. Finally, the formula for the average free energy $\langle F_{SB} \rangle$ takes the form convenient for numerical calculations:

$$
\langle F_{SB} \rangle = \left[\frac{1}{2} K_{33} q_{SB}^2 \theta_{SB}^2 + 2(C_1 + C_2) q_{SB}^4 \theta_{SB}^4 + C_3 q_{SB}^4 \theta_{SB}^4 \right] \frac{1}{N-1} + \sum_{i=1}^{N-2} \left\{ \frac{1}{2} K_{11} q_{SB}^2 \theta_{SB}^2 \cos^2 \frac{2\pi i}{N-1} \sin^2 \left(\theta_{SB} \sin \frac{2\pi i}{N-1} \right) \right.
$$
$$
+ \frac{1}{2} K_{33} q_{SB}^2 \theta_{SB}^2 \cos^2 \frac{2\pi i}{N-1} \cos^2 \left(\theta_{SB} \sin \frac{2\pi i}{N-1} \right) + \frac{1}{2}(C_1 + C_2) \left(q_{SB}^4 \theta_{SB}^2 \sin^2 \frac{2\pi i}{N-1} + 4 q_{SB}^4 \theta_{SB}^4 \cos^4 \frac{2\pi i}{N-1} \right)
$$
$$
+ \frac{1}{4} C_3 \left[4 q_{SB}^4 \theta_{SB}^4 \cos^4 \frac{2\pi i}{N-1} \cos^2 \left(2\theta_{SB} \sin \frac{2\pi i}{N-1} \right) + q_{SB}^4 \theta_{SB}^2 \sin^2 \frac{2\pi i}{N-1} \sin^2 \left(2\theta_{SB} \sin \frac{2\pi i}{N-1} \right) \right.
$$
$$
\left. \left. - 4 q_{SB}^4 \theta_{SB}^3 \cos^2 \frac{2\pi i}{N-1} \sin \frac{2\pi i}{N-1} \cos \left(2\theta_{SB} \sin \frac{2\pi i}{N-1} \right) \sin \left(2\theta_{SB} \sin \frac{2\pi i}{N-1} \right) \right] \right\} \frac{1}{N-1}. \tag{14}
$$

The application of the method of steepest descent to formula (14) enables the computation of equilibrium values of θ_{SB} and q_{SB}.

The calculations are performed for various values of elastic constants in order to determine the dependence of the tilt angle and the wave number on these material parameters. The comparison of the values of f_{TB} and $\langle F_{SB} \rangle$ reveals which liquid-crystalline phase (N_{TB} or N_{SB}) exists in reality for the given set of elastic constants. According to thermodynamics, the structure which is characterized by the lower free energy is stable and appears in experiments.

A. Estimation of the order of magnitude of fourth-order elastic constants

From the theoretical point of view, the order of magnitude of fourth-order elastic constants can be estimated from the approximate formula for the wave number of twist-bend nematics. Simple mathematical transformations of Eq. (5) yields

$$
C_1 + C_2 = -\frac{K_{33}}{3 q_{TB}^2} = -\frac{K_{33} p_{TB}^2}{12 \pi^2}. \tag{15}
$$

According to experimental data, the pitch of twist-bend nematics ranges from 6 to 20 nm [28]. However, for the vast majority of liquid-crystalline compounds exhibiting the N_{TB} phase, the parameter p_{TB} does not exceed 10 nm. CB7CB, which is the most popular dimer forming the twist-bend nematic structure, is characterised by the pitch of 7–8.7 nm [21,29–31]. On this basis it is sensible to assume $p_{TB} \approx 8$ nm for further calculations.

The estimation of the bend elastic constant K_{33} is more problematic. In Dozov's theory this quantity must be negative to ensure the stability of twist-bend nematics. The results of experiments indicate that K_{33} takes small (less than 1 pN) but positive values in the nematic phase, just before the N-N_{TB} transition [32,33]. In the N_{TB} phase the bend elastic constant increases rapidly (for example, from 0.25 pN at 99.6 °C to 47.3 pN at 99.3 °C for CB7CB [34]) when the temperature is decreased. Yun *et al.* try to explain why the measurements do not give negative values of K_{33} [34]. They pay attention to the hierarchical structure of twist-bend nematics. The elastic constants which are determined in the nematic phase just before the N-N_{TB} transition and in the twist-bend nematic phase refer to the distortions of the optic axis **N** treated as a higher-level director. In Dozov's model the elastic constants are connected with the deformations of the molecular level director **n** and therefore they are not measurable. For this reason K_{33} must be estimated from other material parameters. The starting point for further considerations is Eq. (4) which can be rewritten in the equivalent form:

$$
K_{33} = -3 K_{22} \theta_{TB}^2. \tag{16}
$$

It is possible to apply Eq. (16) in the calculations only if the twist elastic constant K_{22} and the tilt angle θ_{TB} are known. The value of K_{22} is a relatively rare subject of research, mainly because of experimental difficulties and high measurement uncertainties. For various liquid-crystalline compounds and their mixtures, K_{22} ranges from 2 to 10 pN in the vicinity of the N-N_{TB} transition [24,33–37]. The results obtained for CB7CB reveal that $K_{22} \approx 5$ pN [34]. This value is often assumed in computations concerning the elastic properties of twist-bend nematics [21]. The theoretical considerations presented by Meyer and Dozov suggest that the twist elastic constants related to the deformations of **n** and **N** are approximately equal [38,39]. This means that the experimental value of K_{22} can be used for the estimation of K_{33}, although the nature of elastic constants obtained from measurements and those from Dozov's model is probably different.

The value of the tilt angle of the N_{TB} phase strongly depends on temperature. According to the results of experiments conducted for CB7CB, this parameter increases from 9° at 101 °C (just below the N-N_{TB} transition) to about 33°–38° at 50 °C [17]. Because other necessary quantities (i.e., the twist elastic constant and the pitch) have been determined for the temperature in the vicinity of the N-N_{TB} transition, the value $\theta_{TB} \approx 9°$ seems appropriate for the further calculations.

Finally, the application of Eqs. (15) and (16) leads to $K_{33} \approx -0.4$ pN and $C_1 + C_2 \approx 2 \times 10^{-31}$ J m. Unfortunately, this simple method based on the approximate formulas given by Dozov does not allow for separate estimation of parameters C_1 and C_2. Nonetheless, the knowledge of the sum $C_1 + C_2$ is

TABLE I. Values of material parameters adopted in the numerical calculations.

Material parameter	Range of values
Twist elastic constant K_{22}	$1 - 10$ pN
Bend elastic constant K_{33}	-5 to -0.1 pN
Fourth-order elastic constant C_1	$0 - 5 \times 10^{-31}$ J m
Fourth-order elastic constant C_2	$0 - 5 \times 10^{-31}$ J m
Fourth-order elastic constant C_3	$0 - 5 \times 10^{-31}$ J m

also extremely useful when numerical calculations concerning twist-bend nematics are planned.

B. Parameters

Table I contains the ranges of values of material parameters which are adopted in the numerical computations conducted for twist-bend nematics and splay-bend nematics.

It is noteworthy that the fourth-order elastic constant C_3 appears only in the calculations concerning the N_{SB} phase [compare Eqs. (9) and (10)]. The splay elastic constant K_{11}, which is not included in Table I, is varied between 0 and the critical value K_{11}^c, for which the difference $\langle F_{SB} \rangle - f_{TB}$ changes the sign from negative to positive. For $K_{11} < K_{11}^c$ the splay-bend nematic phase should be stable. The structure of twist-bend nematics is formed when K_{11} exceeds K_{11}^c. In order to verify the criterion (8), it is necessary to check whether the equality $K_{11}^c = 2K_{22}$ is satisfied.

III. RESULTS

A. Twist-bend nematics

The results of computations indicate that the pitch p_{TB} of twist-bend nematics increases with the values of the fourth-order elastic constants C_1 and C_2, as shown in Fig. 1(a). The analysis of Fig. 1(b) reveals that the tilt angle θ_{TB} does not depend on C_1 when $C_2 = 0$. In other cases θ_{TB} is a decreasing function of C_1. The tilt angle grows when C_2 becomes larger. It should be noted that the variation of θ_{TB} with C_1 and C_2 is weak. This means that the change of the tilt angle does not exceed a few tenths of a degree when the fourth-order elastic constants are varied in the range of $0 - 5 \times 10^{-31}$ J m.
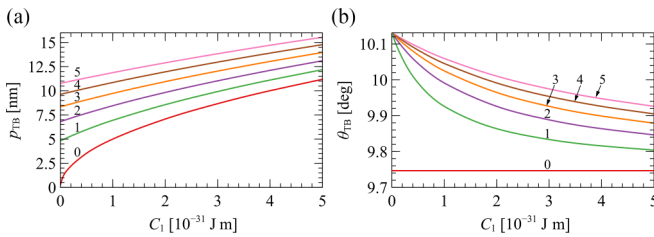

FIG. 1. Pitch p_{TB} (a) and tilt angle θ_{TB} (b) of twist-bend nematics as a function of the fourth-order elastic constant C_1. The curves correspond to the results obtained for different values of the fourth-order elastic constant C_2 which are given in the graphs in 10^{-31} J m. The other material parameters are as follows: $K_{22} = 5$ pN, $K_{33} = -0.5$ pN.
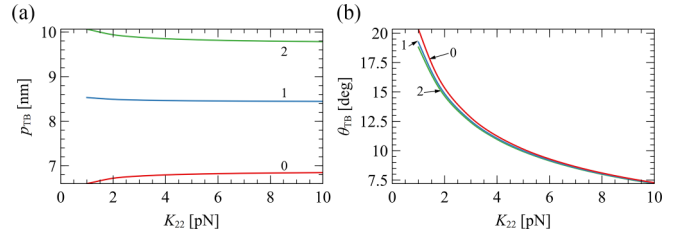

FIG. 2. Pitch p_{TB} (a) and tilt angle θ_{TB} (b) of twist-bend nematics as a function of the twist elastic constant K_{22}. The curves correspond to the results obtained for different values of the fourth-order elastic constant C_1 which are given in the graphs in 10^{-31} J m. The other material parameters are as follows: $K_{33} = -0.5$ pN, $C_2 = 2 \times 10^{-31}$ J m.

The case $C_1 = C_2 = 0$ is not the subject of research because then the free energy density is unbounded from below and does not reach a minimum value. For twist-bend nematics and splay-bend nematics, at least one of the fourth-order elastic constants must be nonzero.

It is apparent from Fig. 2(a) that the value of the twist elastic constant K_{22} does not have a significant influence on the pitch of the N_{TB} structure. The spatial period p_{TB} can either increase or decrease with K_{22}, depending on the value of C_1, but these changes are very subtle. The tilt angle θ_{TB} gets smaller when K_{22} is increased. The results presented in Fig. 2(b) confirm that the dependence of θ_{TB} on the fourth-order elastic C_1 is really weak.

When the bend elastic constant K_{33} becomes more negative, the pitch of the N_{TB} phase declines, whereas the tilt angle rises, as demonstrated in Fig. 3. It is obvious that the negative values of K_{33} stimulate the formation of a twist-bend nematic structure. The detailed analysis indicates that the approximate formula (5) gives acceptable values of p_{TB}, which differ from those obtained numerically by no more than 5% in the majority of cases. Figure 3(b) suggests that the situation looks totally different for the tilt angle. Indeed, the difference between the numerical value of θ_{TB} and that calculated from Eq. (4) can surpass 30% for some sets of material parameters. Such considerable divergences occur when K_{33} is smaller than
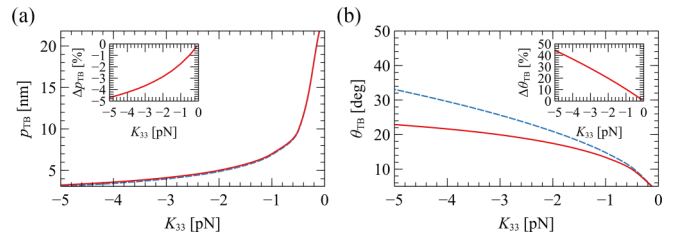

FIG. 3. Pitch p_{TB} (a) and tilt angle θ_{TB} (b) of twist-bend nematics as a function of the bend elastic constant K_{33}. The solid lines correspond to the results p_{TB}^n and θ_{TB}^n obtained by means of numerical calculations. The dashed curves have been plotted on the basis of values p_{TB}^f and θ_{TB}^f calculated from Eqs. (4) and (5). The insets present how the percentage differences $\Delta p_{TB} = [(p_{TB}^f - p_{TB}^n)/p_{TB}^n] \times 100\%$ and $\Delta \theta_{TB} = [(\theta_{TB}^f - \theta_{TB}^n)/\theta_{TB}^n] \times 100\%$ depend on K_{33}. The other material parameters are as follows: $K_{22} = 5$ pN, $C_1 = C_2 = 2 \times 10^{-31}$ J m. In (a) the solid curve and the dashed one almost overlap.

−3 pN and consequently θ_{TB} takes relatively large values exceeding 20°. These results are consistent with expectations since Dozov derived the formulas (4) and (5) assuming small values of the tilt angle.

According to the results of numerical computations, the pitch of the N_{TB} phase depends on K_{22} and the tilt angle is a function of C_1 and C_2, although Eqs. (4) and (5) exclude such relations. This raises a question of whether it is possible to determine more accurate formulas for q_{TB} and θ_{TB} in the frame of Dozov's theory. The answer is affirmative. The application of standard methods of multivariable calculus to Eq. (9) leads to the following results:

$$q_{TB} = \pm\sqrt{\frac{-3(C_1 + C_2)(K_{33} - K_{22}) - \sqrt{(C_1 + C_2)(K_{33} - K_{22})[9(C_1 + C_2)(K_{33} - K_{22}) - 8K_{33}(C_2 - 3C_1)]}}{4(C_1 + C_2)(C_2 - 3C_1)}}, \quad (17)$$

$$\sin^2\theta_{TB} = \frac{3(C_1 + C_2)(K_{33} - K_{22}) + \sqrt{(C_1 + C_2)(K_{33} - K_{22})[9(C_1 + C_2)(K_{33} - K_{22}) - 8K_{33}(C_2 - 3C_1)]}}{4(C_2 - 3C_1)(K_{33} - K_{22})}. \quad (18)$$

It must be emphasized that Eqs. (17) and (18) have been derived without making any redundant simplifications. The wave number of twist-bend nematics can be positive or negative for the right-handed and left-handed structures, respectively.

When the fourth-order elastic constants satisfy the condition $C_2 - 3C_1 = 0$, Eqs. (17) and (18) cannot be used any longer. The calculations show that in this specific case the formulas for q_{TB} and θ_{TB} take the following form:

$$q_{TB} = \pm\sqrt{\frac{-K_{33}}{3(C_1 + C_2)}}, \quad (19)$$

$$\sin^2\theta_{TB} = \frac{K_{33}}{3(K_{33} - K_{22})}. \quad (20)$$

It is provable that Eqs. (17)–(20) really correspond to the minimum of the free energy density. Not only is the gradient of (9) equal to zero, but also the Hessian matrix is positive definite for q_{TB} and θ_{TB} given by Eqs. (17)–(20). It has been assumed that the material parameters fulfill the standard criteria ($K_{22} > 0$, $K_{33} < 0$, $C_1 \geqslant 0$, $C_2 \geqslant 0$, $C_1 + C_2 > 0$). Under these assumptions, the values of $\sin^2\theta$ calculated from Eqs. (18) and (20) meet the necessary conditions $\sin^2\theta_{TB} > 0$ and $\sin^2\theta_{TB} < 1$. These inequalities do not impose any additional restrictions on the elastic constants.

The situation when one of the fourth-order elastic constants is equal to zero deserves separate consideration. For $C_1 = 0$, Eqs. (17) and (18) can be rewritten as follows:

$$q_{TB} = \pm\sqrt{\frac{-3(K_{33} - K_{22}) - \sqrt{(K_{33} - K_{22})(K_{33} - 9K_{22})}}{4C_2}}, \quad (21)$$

$$\sin^2\theta_{TB} = \frac{3(K_{33} - K_{22}) + \sqrt{(K_{33} - K_{22})(K_{33} - 9K_{22})}}{4(K_{33} - K_{22})}. \quad (22)$$

When $C_2 = 0$, the wave number of twist-bend nematics and the tilt angle can be calculated from the following formulas:

$$q_{TB} = \pm\sqrt{\frac{3(K_{33} - K_{22}) + \sqrt{(K_{33} - K_{22})(33K_{33} - 9K_{22})}}{12C_1}}, \quad (23)$$

$$\sin^2\theta_{TB} = \frac{-3(K_{33} - K_{22}) - \sqrt{(K_{33} - K_{22})(33K_{33} - 9K_{22})}}{12(K_{33} - K_{22})}. \quad (24)$$

The analysis of Eqs. (22) and (24) reveals that the tilt angle does not depend on the value of C_2 when $C_1 = 0$. Analogously, θ_{TB} does not vary with C_1 for $C_2 = 0$. Similar conclusions have been formulated on the basis of results of numerical calculations. Generally, the values of q_{TB} and θ_{TB} obtained numerically are closely akin to those calculated from Eqs. (17)–(20).
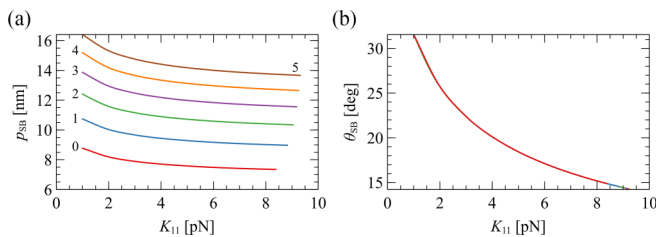

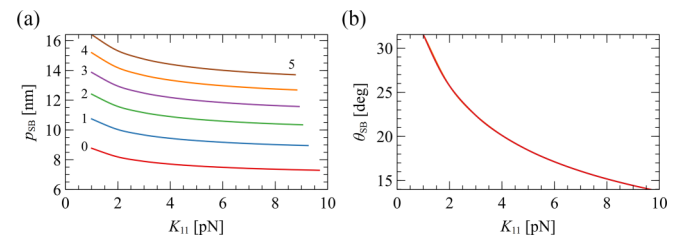FIG. 4. Spatial period p_{SB} (a) and tilt angle θ_{SB} (b) of splay-bend nematics as a function of the splay elastic constant K_{11}. The curves correspond to the results obtained for different values of the fourth-order elastic constant C_1 which are given in the graphs in 10^{-31} J m. The other material parameters are as follows: $K_{22} = 5$ pN, $K_{33} = -0.5$ pN, $C_2 = 2 \times 10^{-31}$ J m, $C_3 = 0$. In (b) the curves overlap.

FIG. 5. Spatial period p_{SB} (a) and tilt angle θ_{SB} (b) of splay-bend nematics as a function of the splay elastic constant K_{11}. The curves correspond to the results obtained for different values of the fourth-order elastic constant C_2 which are given in the graphs in 10^{-31} J m. The other material parameters are as follows: $K_{22} = 5$ pN, $K_{33} = -0.5$ pN, $C_1 = 2 \times 10^{-31}$ J m, $C_3 = 0$. In (b) the curves overlap.
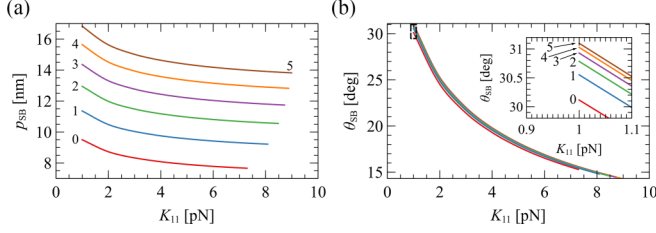
FIG. 6. Spatial period p_{SB} (a) and tilt angle θ_{SB} (b) of splay-bend nematics as a function of the splay elastic constant K_{11}. The curves correspond to the results obtained for different values of the fourth-order elastic constant C_1 which are given in the graphs in 10^{-31} J m. The other material parameters are as follows: $K_{22} = 5$ pN, $K_{33} = -0.5$ pN, $C_2 = C_3 = 2 \times 10^{-31}$ J m. The inset in (b) shows the enlargement of the region bounded by the dashed rectangle.

FIG. 7. Spatial period p_{SB} (a) and tilt angle θ_{SB} (b) of splay-bend nematics as a function of the splay elastic constant K_{11}. The curves correspond to the results obtained for different values of the fourth-order elastic constant C_2 which are given in the graphs in 10^{-31} J m. The other material parameters are as follows: $K_{22} = 5$ pN, $K_{33} = -0.5$ pN, $C_1 = C_3 = 2 \times 10^{-31}$ J m. The inset in (b) shows the enlargement of the region bounded by the dashed rectangle.

The formulas (4) and (5) given by Dozov can be obtained from the linear approximation of Eqs. (17) and (18) in the vicinity of $K_{33} = 0$. The expressions for q_{TB} and $\sin^2\theta_{TB}$ must be treated as functions of the bend elastic constant K_{33} and expanded into power series up to terms proportional to K_{33}:

$$q_{TB}(K_{33}) \approx q_{TB}(0) + K_{33} \left.\frac{\partial q_{TB}}{\partial K_{33}}\right|_{K_{33}=0}, \quad (25)$$

$$\sin^2\theta_{TB}(K_{33}) \approx \sin^2\theta_{TB}(0) + K_{33} \left.\frac{\partial(\sin^2\theta_{TB})}{\partial K_{33}}\right|_{K_{33}=0}. \quad (26)$$

The further calculations yield

$$q_{TB}(0) = 0, \quad \left.\frac{\partial q_{TB}}{\partial K_{33}}\right|_{K_{33}=0} = -\frac{1}{3(C_1 + C_2)},$$

$$\sin^2\theta_{TB}(0) = 0, \quad \left.\frac{\partial(\sin^2\theta_{TB})}{\partial K_{33}}\right|_{K_{33}=0} = -\frac{1}{3K_{22}}. \quad (27)$$

Taking these results into account and assuming the approximation of small angles $\sin^2\theta_{TB} \approx \theta_{TB}^2$, one can redetermine Eqs. (4) and (5) presented by Dozov. These formulas are applicable when K_{33} is slightly less than 0. The identical conclusion has been drawn from the output of numerical computations [see Fig. 3(b)].

B. Splay-bend nematics

The results of numerical calculations indicate that the spatial period p_{SB} of the N_{SB} phase and the tilt angle θ_{SB} decrease with the splay elastic constant K_{11}. The value of p_{SB} grows when the fourth-order elastic constants C_1 and C_2 are increased [Figs. 4(a), 5(a), 6(a), and 7(a)]. For $C_3 = 0$ the tilt angle θ_{SB} does not vary with C_1 and C_2, as is visible in Figs. 4(b) and 5(b). When $C_3 \neq 0$, θ_{SB} becomes an increasing function of C_1 and C_2, although Figs. 6(b) and 7(b) reveal that this dependence is very weak.

The in-depth analysis shows that the mutual interchange of C_1 and C_2 alters neither the spatial period nor the tilt angle of the N_{SB} phase. However, the stability ranges of splay-bend nematics are different in these two cases. This fact can be easily explained. According to Eq. (9), the interchange of constants C_1 and C_2 in the case of the N_{TB} structure leads to different values of the free energy. For this reason the
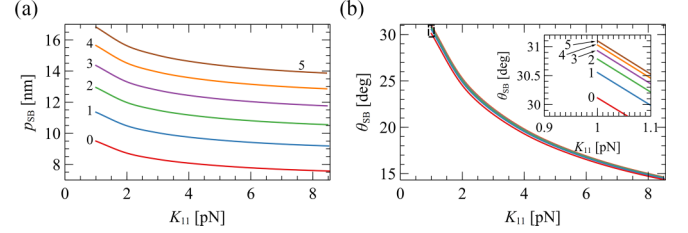
difference $\langle F_{SB} \rangle - f_{TB}$ becomes zero for different values of K_{11} in both considered cases. In this way the stability ranges of the N_{SB} phase are not the same when the values of C_1 and C_2 are swapped.

The twist deformation does not appear in the N_{SB} phase and therefore the values of p_{SB} and θ_{SB} do not depend on the twist elastic constant K_{22}. On the other hand, the negative value of the bend elastic constant K_{33} has considerable influence on the quantities characterizing splay-bend nematics. When the absolute value of K_{33} becomes larger, the spatial period declines and the tilt angle increases, as presented in Fig. 8. This effect (similar to that observed for twist-bend nematics) is understandable because the negative value of K_{33} favors the appearance of spontaneous bend deformations and thus the periodically modulated nematic structure can be formed.

The results shown in Fig. 9 indicate that the spatial period of splay-bend nematics rises with the fourth-order elastic constant C_3 and simultaneously the tilt angle decreases. The changes of p_{SB} and θ_{SB} are relatively small in this situation. It can be supposed that the term with C_3 in the formula (10) for the free energy density inhibits the formation of the N_{SB} structure.

In most cases the values of p_{SB} and θ_{SB} obtained as a result of numerical calculations are clearly different from those calculated from Eqs. (6) and (7) given by Dozov. The N_{SB} structure is usually characterized by the large tilt angle and for this reason the approximate formulas give extremely
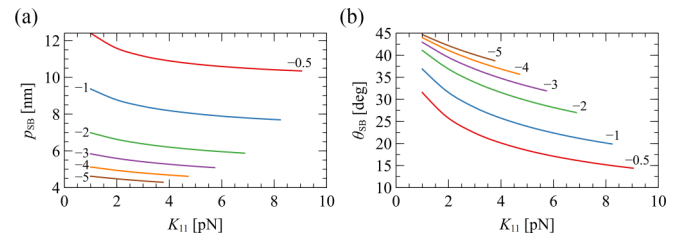

FIG. 8. Spatial period p_{SB} (a) and tilt angle θ_{SB} (b) of splay-bend nematics as a function of the splay elastic constant K_{11}. The curves correspond to the results obtained for different values of the bend elastic constant K_{33} which are given in the graphs in pN. The other material parameters are as follows: $K_{22} = 5$ pN, $C_1 = C_2 = 2 \times 10^{-31}$ J m, $C_3 = 0$.

(a)   (b)   (a)   (b)
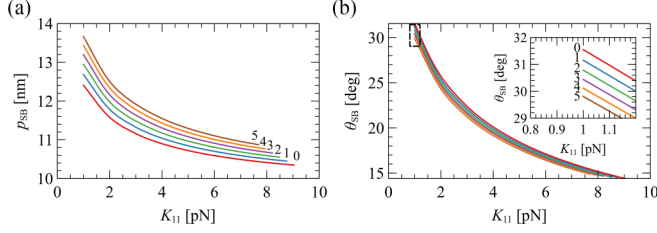
FIG. 9. Spatial period p_{SB} (a) and tilt angle θ_{SB} (b) of splay-bend nematics as a function of the splay elastic constant K_{11}. The curves correspond to the results obtained for different values of the fourth-order elastic constant C_3 which are given in the graphs in 10^{-31} J m. The other material parameters are as follows: $K_{22} = 5$ pN, $K_{33} = -0.5$ pN, $C_1 = C_2 = 2 \times 10^{-31}$ J m. The inset in (b) shows the enlargement of the region bounded by the dashed rectangle.

inaccurate results. Generally, the values of the tilt angle calculated from Eq. (6) are overestimated in comparison to the outcome of numerical computations, whereas Eq. (7) yields too low values of the pitch. Figure 10 presents that the congruence between the values calculated from the approximate formulas and those obtained numerically is quite good if the tilt angle is sufficiently small. This situation takes place when K_{33} is slightly less than 0 and K_{11} approaches the critical value K_{11}^c.
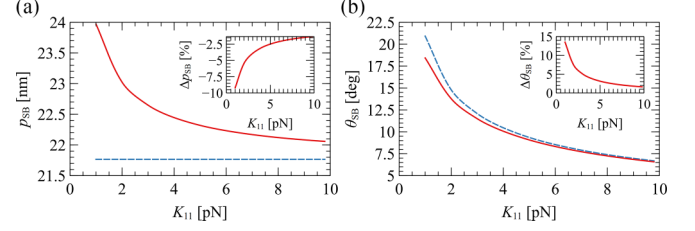
FIG. 10. Spatial period p_{SB} (a) and tilt angle θ_{SB} (b) of splay-bend nematics as a function of the splay elastic constant K_{11}. The solid lines correspond to the results p_{SB}^n and θ_{SB}^n obtained by means of numerical calculations. The dashed curves have been plotted on the basis of values p_{SB}^f and θ_{SB}^f calculated from Eqs. (6) and (7). The insets present how the percentage differences $\Delta p_{SB} = [(p_{SB}^f - p_{SB}^n)/p_{SB}^n] \times 100\%$ and $\Delta\theta_{SB} = [(\theta_{SB}^f - \theta_{SB}^n)/\theta_{SB}^n] \times 100\%$ depend on K_{11}. The other material parameters are as follows: $K_{22} = 5$ pN, $K_{33} = -0.1$ pN, $C_1 = C_2 = 2 \times 10^{-31}$ J m, $C_3 = 0$.

Unfortunately, it is not possible to determine the exact formulas for p_{SB} and θ_{SB}, because Eq. (10) is too complicated. The analytical integration of f_{SB} over one period of the N_{SB} structure seems unfeasible. However, one can derive approximate formulas for p_{SB} and θ_{SB} which give more accurate results than those proposed by Dozov. For this purpose, f_{SB} must be expanded into series up to θ_{SB}^4 terms:

$$f_{SB}^{IV} = \frac{\left[(C_2 + C_1)q_{SB}^4 \sin^2 q_{SB}z + K_{33}q_{SB}^2\cos^2 q_{SB}z\right]\theta_{SB}^2}{2}$$
$$+ \frac{\left\{2C_3 q_{SB}^4\sin^4 q_{SB}z - \left[4C_3 q_{SB}^4 + (K_{33} - K_{11})q_{SB}^2\right]\cos^2 q_{SB}z\sin^2 q_{SB}z + (2C_3 + 4C_2 + 4C_1)q_{SB}^4\cos^4 q_{SB}z\right\}\theta_{SB}^4}{2}. \quad (28)$$

Now the formula (28) can be averaged over one period of the N_{SB} structure without any problems. The result of this operation is as follows:

$$\langle f_{SB}^{IV}\rangle = \frac{\left[4(2C_3 + 3C_2 + 3C_1)q_{SB}^4 + (K_{11} - K_{33})q_{SB}^2\right]\theta_{SB}^4 + 4\left[(C_2 + C_1)q_{SB}^4 + K_{33}q_{SB}^2\right]\theta_{SB}^2}{16}. \quad (29)$$

The minimization of Eq. (29) yields the equilibrium values of q_{SB}^2 and θ_{SB}^2:

$$q_{SB}^2 = \frac{3(C_2 + C_1)(K_{33} - K_{11}) + \sqrt{(C_2 + C_1)(K_{33} - K_{11})[(64C_3 + 105C_1 + 105C_2)K_{33} - 9(C_2 + C_1)K_{11}]}}{16(C_2 + C_1)(2C_3 + 3C_2 + 3C_1)}, \quad (30)$$

$$\theta_{SB}^2 = \frac{3(C_2 + C_1)(K_{33} - K_{11}) + \sqrt{(C_2 + C_1)(K_{33} - K_{11})[(64C_3 + 105C_1 + 105C_2)K_{33} - 9(C_2 + C_1)K_{11}]}}{4(2C_3 + 3C_2 + 3C_1)(K_{11} - K_{33})}. \quad (31)$$

According to the results of computations, the average difference between the value calculated from Eqs. (30) or (31) and that obtained numerically is equal to 2%. This fact proves the usefulness of the derived formulas, although their mathematical form is quite complex and therefore inconvenient for calculations. When $C_3 = 0$, Eq. (31) takes the form

$$\theta_{SB}^2 = \frac{-3(K_{11} - K_{33}) + \sqrt{3(K_{11} - K_{33})(3K_{11} - 35K_{33})}}{12(K_{11} - K_{33})}, \quad (32)$$

which confirms that in this particular situation the tilt angle of the N_{SB} phase does not depend on the values of the fourth-order elastic constants C_1 and C_2. Similarly as in the case of

twist-bend nematics, it can be shown that Dozov's formulas (6) and (7) are the linear approximation of Eqs. (30) and (31) in the vicinity of $K_{33} = 0$.

C. Critical value K_{11}^c

The results of numerical calculations indicate that the critical value K_{11}^c is not simply expressed by the formula $K_{11}^c = 2K_{22}$ derived by Dozov. It turns out that various material parameters influence K_{11}^c. Figure 11 illustrates that K_{11}^c actually increases linearly with K_{22}; however, the critical values obtained numerically are smaller than those calculated from Dozov's formula. When the bend elastic constant K_{33} becomes
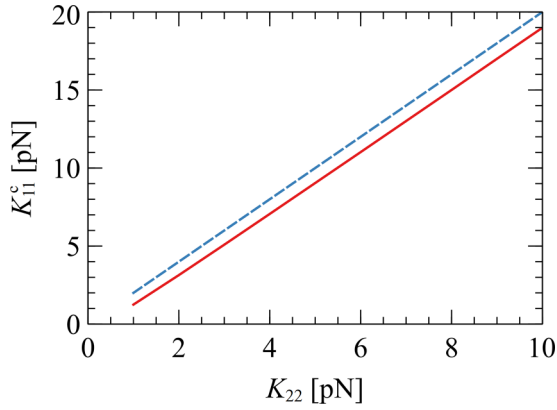
FIG. 11. Critical value K_{11}^c as a function of the twist elastic constant K_{22}. The solid line corresponds to the results obtained by means of numerical calculations. The dashed line has been plotted on the basis of values calculated from the formula $K_{11}^c = 2K_{22}$ given by Dozov. The other material parameters are as follows: $K_{33} = -0.5$ pN, $C_1 = C_2 = 2 \times 10^{-31}$ J m, $C_3 = 0$.

less negative, K_{11}^c grows, as shown in Fig. 12. It is evident that K_{11}^c tends to $2K_{22}$ as K_{33} approaches zero. This means that Dozov's criterion (8) for the stability of twist-bend nematics is applicable when K_{33} is slightly negative.

There is no doubt that the relationship between K_{11}^c and fourth-order elastic constants C_1, C_2, C_3 is complicated. Figure 13 presents how K_{11}^c depends on C_1 and C_2 when $C_3 = 0$. The critical value does not vary with C_2 when $C_1 = 0$ and it is independent of C_1 for $C_2 = 0$. The critical value declines when C_1 is positive and C_2 becomes larger. The increase of C_1 leads to the growth of K_{11}^c.

When C_3 is nonzero, K_{11}^c can be either an increasing or decreasing function of C_2 and this depends on the value of C_1, as shown in Fig. 14. It is worth noticing that K_{11}^c varies with C_2 when $C_1 = 0$, so this behavior is different from that observed in the analogous case with $C_3 = 0$. The critical value increases with C_1, even when $C_2 = 0$, and decreases linearly with C_3 (Fig. 15).

FIG. 13. Critical value K_{11}^c as a function of the fourth-order elastic constant C_2. The curves correspond to the results obtained for different values of the fourth-order elastic constant C_1 which are given in the graph in 10^{-31} J m. The other material parameters are as follows: $K_{22} = 5$ pN, $K_{33} = -0.5$ pN, $C_3 = 0$.

According to the results presented in Fig. 16, the material parameters can be chosen so that the N_{TB} phase is stable for any positive value of the splay elastic constant K_{11}. For instance, this situation takes place when $K_{22} = 5$ pN, $C_1 = C_3 = 0$, $C_2 = 2 \times 10^{-31}$ J m, and $K_{33} < -4.2$ pN. Of course, it is possible to show that the N_{SB} structure can appear for some negative values of K_{11} in these cases. However, the negative values of any elastic constant are hard to interpret. Their introduction always provokes major controversy; hence this operation should be preceded by in-depth theoretical and experimental research.

IV. CONCLUSIONS

The results of numerical calculations demonstrate the complex influence of material parameters on the quantities characterizing the structure of twist-bend nematics and splay-bend nematics, namely, the tilt angle θ_{TB} (or θ_{SB}), the pitch p_{TB}, and
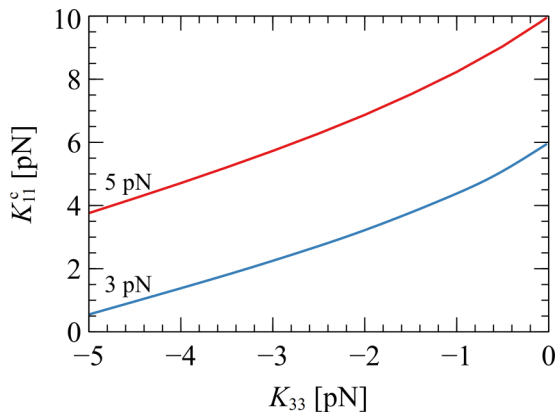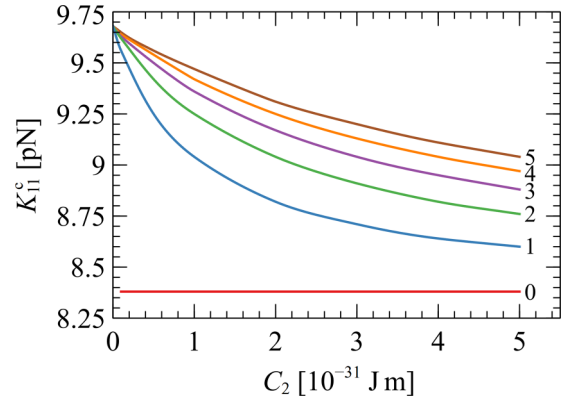

FIG. 12. Critical value K_{11}^c as a function of the bend elastic constant K_{33}. The curves correspond to the results obtained for different values of the twist elastic constant K_{22} which are given in the graph. The other material parameters are as follows: $C_1 = C_2 = 2 \times 10^{-31}$ J m, $C_3 = 0$.

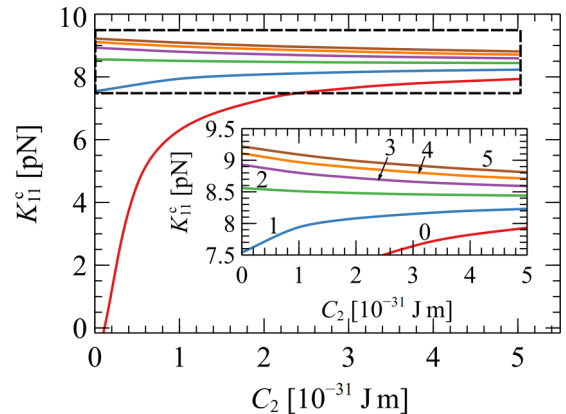

FIG. 14. Critical value K_{11}^c as a function of the fourth-order elastic constant C_2. The curves correspond to the results obtained for different values of the fourth-order elastic constant C_1 which are given in the graph in 10^{-31} J m. The other material parameters are as follows: $K_{22} = 5$ pN, $K_{33} = -0.5$ pN, $C_3 = 2 \times 10^{-31}$ J m. The inset presents the enlargement of the region bounded by the dashed rectangle.
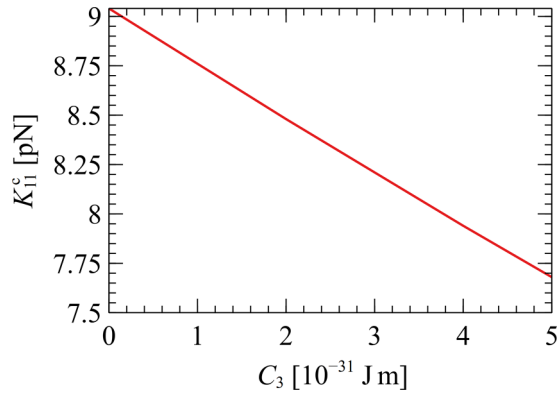
FIG. 15. Critical value K_{11}^c as a function of the fourth-order elastic constant C_3. The other material parameters are as follows: $K_{22} = 5$ pN, $K_{33} = -0.5$ pN, $C_1 = C_2 = 2 \times 10^{-31}$ J m.

the spatial period p_{SB}. The critical value K_{11}^c, which separates the ranges of stability of splay-bend nematics and twist-bend nematics, is also strongly dependent on the values of elastic constants. It must be emphasized that the values of K_{11}^c obtained numerically are smaller than those calculated from Dozov's formula $K_{11}^c = 2K_{22}$. The experiments conducted by Yun *et al.* actually confirm that the N_{TB} phase can be formed when K_{11} is much less than $2K_{22}$ [34]. The scientists try to clarify the differences between the results of measurements and the theory by means of the hierarchical structure of twist-bend nematics. However, it should be remembered that Dozov's criterion (8) is only an approximation with limited applicability and this may be the additional source of discrepancies.

The formulas for parameters characterizing the structure of twist-bend nematics or splay-bend nematics have complicated mathematical form and they differ from those given by Dozov. Unfortunately, the exact formulas can be derived without any simplifications only for the N_{TB} phase. For the N_{SB} structure the formula for the free energy density must be approximated by a truncated power series. Only then can the values of the spatial period p_{SB} and the tilt angle θ_{SB} be determined analytically. The formulas (30) and (31) are helpful when there is no possibility of performing numerical computations and one wants to estimate the values of p_{SB} and θ_{SB}.

The separate estimation of the fourth-order elastic constants C_1, C_2, C_3 is not possible on the basis of approximate formulas given by Dozov. The simple calculations have revealed that the sum $C_1 + C_2$ is of the order of 10^{-31} J m. There is no doubt that further research should be directed towards the experimental determination of material parameters of liquid crystals exhibiting novel modulated nematic phases. The exact values of elastic constants are essential for conducting reliable simulations of twist-bend nematics or splay-bend nematics. However, the measurement of these parameters is problematic
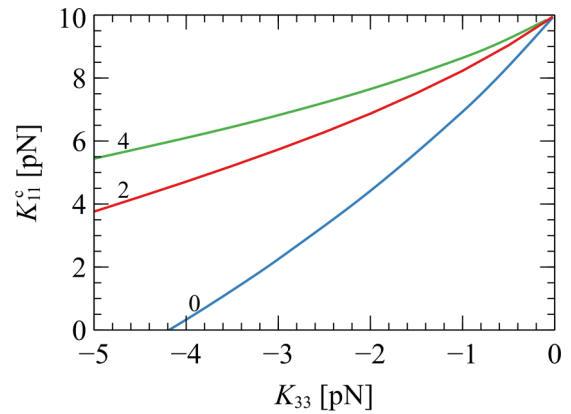

FIG. 16. Critical value K_{11}^c as a function of the bend elastic constant K_{33}. The curves correspond to the results obtained for different values of the fourth-order elastic constant C_1 which are given in the graph in 10^{-31} J m. The other material parameters are as follows: $K_{22} = 5$ pN, $C_2 = 2 \times 10^{-31}$ J m, $C_3 = 0$.

and affected by significant uncertainties, mainly because of the nature of elastic continuum theories. The experimental setup must be designed specifically for a given theory and the values of elastic constants also depend on the chosen model. The current research on this subject is definitely not sufficient.

In the future it would be a good idea to perform similar numerical computations on the basis of other elasticity models, for example, those proposed by Shamid *et al.* [19] or Barbero *et al.* [23]. In this way the relationship between elastic constants appearing in various theories could be recognized. Moreover, new elasticity theories containing the smallest possible number of material parameters would be helpful.

It is not feasible to conduct numerical calculations for all possible combinations of values of material parameters. It is not excluded that the final conclusions (for example, those concerning the behavior of the tilt angle or the pitch on the variation of elastic constants) could be slightly different if the computations were performed for other values of material parameters. Nevertheless, the results presented in this paper help researchers to gain a general understanding of the role of elastic constants appearing in Dozov's theory. Moreover, it is hoped that the outcome of this research will facilitate the search for thermotropic liquid crystals exhibiting the N_{SB} phase.

[1] R. B. Meyer, Structural problems in liquid crystals physics, in *Molecular Fluids*, edited by R. Balian and G. Weill (Gordon and Breach Science Publishers, London, 1976), pp. 271–343.

[2] I. Dozov, On the spontaneous symmetry breaking in the mesophases of achiral banana-shaped molecules, Europhys. Lett. **56**, 247 (2001).

[3] R. Memmer, Liquid crystal phases of achiral banana-shaped molecules: A computer simulation study, Liq. Cryst. **29**, 483 (2002).

[4] C. Meyer, G. R. Luckhurst, and I. Dozov, Flexoelectrically driven electroclinic effect in the twist-bend nematic phase of achiral molecules with bent shapes, Phys. Rev. Lett. **111**, 067801 (2013).

[5] P. K. Challa, V. Borshch, O. Parri, C. T. Imrie, S. N. Sprunt, J. T. Gleeson, O. D. Lavrentovich, and A. Jákli, Twist-bend nematic liquid crystals in high magnetic fields, Phys. Rev. E **89**, 060501(R) (2014).

[6] M. Cestari *et al.*, Phase behavior and properties of the liquid-crystal dimer 1″,7″-bis(4-cyanobiphenyl-4′-yl) heptane: A twist-bend nematic liquid crystal, Phys. Rev. E **84**, 031704 (2011).

[7] B. Robles-Hernández, N. Sebastián, M. R. de la Fuente, D. O. López, S. Diez-Berart, J. Salud, M. B. Ros, D. A. Dunmur, G. R. Luckhurst, and B. A. Timimi, Twist, tilt, and orientational order at the nematic to twist-bend nematic phase transition of 1″,9″-bis(4-cyanobiphenyl-4′-yl) nonane: A dielectric, ^{2}H NMR, and calorimetric study, Phys. Rev. E **92**, 062505 (2015).

[8] D. A. Paterson *et al.*, Understanding the twist-bend nematic phase: The characterisation of 1-(4-cyanobiphenyl-4′-yloxy)-6-(4-cyanobiphenyl-4′-yl)hexane (CB6OCB) and comparison with CB7CB, Soft Matter **12**, 6827 (2016).

[9] G. Babakhanova, H. Wang, M. Rajabi, D. Li, Q. Li, and O. D. Lavrentovich, Elastic and electro-optical properties of flexible fluorinated dimers with negative dielectric anisotropy, Liq. Cryst. **49**, 982 (2022).

[10] E. T. Samulski, A. G. Vanakaras, and D. J. Photinos, The twist bend nematic: A case of mistaken identity, Liq. Cryst. **47**, 2092 (2020).

[11] E. T. Samulski, The ever elusive, yet-to-be-discovered twist-bend nematic phase, Crystals **13**, 1648 (2023).

[12] I. Dozov and G. R. Luckhurst, Setting things straight in 'The twist-bend nematic: A case of mistaken identity', Liq. Cryst. **47**, 2098 (2020).

[13] G. Pająk, L. Longa, and A. Chrzanowska, Nematic twist-bend phase in an external field, Proc. Natl. Acad. Sci. USA **115**, E10303 (2018).

[14] K. Merkel, A. Kocot, J. K. Vij, and G. Shanker, Distortions in structures of the twist bend nematic phase of a bent-core liquid crystal by the electric field, Phys. Rev. E **98**, 022704 (2018).

[15] C. Meyer, C. Blanc, G. R. Luckhurst, P. Davidson, and I. Dozov, Biaxiality-driven twist-bend to splay-bend nematic phase transition induced by an electric field, Sci. Adv. **6**, eabb8212 (2020).

[16] C. Fernández-Rico, M. Chiappini, T. Yanagishima, H. de Sousa, D. G. A. L. Aarts, M. Dijkstra, and R. P. A. Dullens, Shaping colloidal bananas to reveal biaxial, splay-bend nematic, and smectic phases, Science **369**, 950 (2020).

[17] C. Meyer, G. R. Luckhurst, and I. Dozov, The temperature dependence of the heliconical tilt angle in the twist-bend nematic phase of the odd dimer CB7CB, J. Mater. Chem. C **3**, 318 (2015).

[18] M. Szmigielski, Theoretical models of modulated nematic phases, Soft Matter **19**, 2675 (2023).

[19] S. M. Shamid, S. Dhakal, and J. V. Selinger, Statistical mechanics of bend flexoelectricity and the twist-bend phase in bent-core liquid crystals, Phys. Rev. E **87**, 052503 (2013).

[20] Z. Parsouzi *et al.*, Fluctuation modes of a twist-bend nematic liquid crystal, Phys. Rev. X **6**, 021041 (2016).

[21] C. Meyer, Nematic twist-bend phase under external constraints, Liq. Cryst. **43**, 2144 (2016).

[22] E. G. Virga, Double-well elastic theory for twist-bend nematic phases, Phys. Rev. E **89**, 052502 (2014).

[23] G. Barbero, L. R. Evangelista, M. P. Rosseto, R. S. Zola, and I. Lelidis, Elastic continuum theory: Towards understanding of the twist-bend nematic phases, Phys. Rev. E **92**, 030501(R) (2015).

[24] M. Čopič and A. Mertelj, Q-tensor model of twist-bend and splay nematic phases, Phys. Rev. E **101**, 022704 (2020).

[25] N. Vaupotič, M. Čepič, M. A. Osipov, and E. Gorecka, Flexoelectricity in chiral nematic liquid crystals as a driving mechanism for the twist-bend and splay-bend modulated phases, Phys. Rev. E **89**, 030501(R) (2014).

[26] E. I. Kats and V. V. Lebedev, Landau theory for helical nematic phases, JETP Lett. **100**, 110 (2014).

[27] E. K. Chong and S. H. Żak, Gradient methods, *An Introduction to Optimization*, 2nd ed. (John Wiley & Sons, Inc., New York, 2001), pp. 113–138.

[28] R. Saha, C. Feng, C. Welch, G. H. Mehl, J. Feng, C. Zhu, J. Gleeson, S. Sprunt, and A. Jákli, The interplay between spatial and heliconical bond order in twist-bend nematic materials, Phys. Chem. Chem. Phys. **23**, 4055 (2021).

[29] M. Salamończyk, N. Vaupotič, D. Pociecha, C. Wang, C. Zhu, and E. Gorecka, Structure of nanoscale-pitch helical phases: Blue phase and twist-bend nematic phase resolved by resonant soft x-ray scattering, Soft Matter **13**, 6694 (2017).

[30] D. Chen *et al.*, Chiral heliconical ground state of nanoscale pitch in a nematic liquid crystal of achiral molecular dimers, Proc. Natl. Acad. Sci. USA **110**, 15931 (2013).

[31] V. Borshch *et al.*, Nematic twist-bend phase with nanoscale modulation of molecular orientation, Nat. Commun. **4**, 2635 (2013).

[32] N. Sebastián, B. Robles-Hernández, S. Diez-Berart, J. Salud, G. R. Luckhurst, D. A. Dunmur, D. O. López, and M. R. de la Fuente, Distinctive dielectric properties of nematic liquid crystal dimers, Liq. Cryst. **44**, 177 (2017).

[33] G. Babakhanova, Z. Parsouzi, S. Paladugu, H. Wang, Y. A. Nastishin, S. V. Shiyanovskii, S. Sprunt, and O. D. Lavrentovich, Elastic and viscous properties of the nematic dimer CB7CB, Phys. Rev. E **96**, 062704 (2017).

[34] C. J. Yun, M. R. Vengatesan, J. K. Vij, and J. K. Song, Hierarchical elasticity of bimesogenic liquid crystals with twist-bend nematic phase, Appl. Phys. Lett. **106**, 173102 (2015).

[35] G. Cukrov, Y. Mosaddeghian Golestani, J. Xiang, Y. A. Nastishin, Z. Ahmed, C. Welch, G. H. Mehl, and O. D. Lavrentovich, Comparative analysis of anisotropic material properties of uniaxial nematics formed by flexible dimers and rod-like monomers, Liq. Cryst. **44**, 219 (2017).

[36] Z. Parsouzi *et al.*, Pretransitional behavior of viscoelastic parameters at the nematic to twist-bend nematic phase transition in flexible *n*-mers, Phys. Chem. Chem. Phys. **21**, 13078 (2019).

[37] K. Adlem, M. Čopič, G. R. Luckhurst, A. Mertelj, O. Parri, R. M. Richardson, B. D. Snow, B. A. Timimi, R. P. Tuffin, and D. Wilkes, Chemically induced twist-bend nematic liquid crystals, liquid crystal dimers, and negative elastic constants, Phys. Rev. E **88**, 022503 (2013).

[38] C. Meyer and I. Dozov, Local distortion energy and coarse-grained elasticity of the twist-bend nematic phase, Soft Matter **12**, 574 (2016).

[39] I. Dozov and C. Meyer, Analogy between the twist-bend nematic and the smectic A phases and coarse-grained description of the macroscopic N_{TB} properties, Liq. Cryst. **44**, 4 (2017).